J. Braz. Chem. Soc., Vol. 9, No. 1, 31-38, 1998.
Printed in Brazil.

0103 – 5053 $6.00 + 0.00

Article

A Study of the Underpotential Deposition of Lead on Gold by UV-Visible Differential Reflectance Spectroscopy

Artur J. Motheo[a]*, Ernesto R. Gonzalez[a], Germano Tremilliosi-Filho[a], André Rakotondrainibe[b], Jean-Michel Léger[b], Bernard Beden[b], and Claude Lamy[b]

[a]*Instituto de Química de São Carlos, Universidade de São Paulo, C.P. 780, 13560-970 São Carlos - SP, Brazil*

[b]*Laboratoire de Chimie 1, "Electrochimie et Interactions" URA CNRS 350 Université de Poitiers, 40, Avenue du Recteur Pineau, 86022 Poitiers Cedex, France*

Received: November 26, 1996

A deposição, em regime de sub-tensão, de chumbo sobre ouro, foi estudada por voltametria cíclica e espectroscopia de reflectância diferencial no domínio UV-visível. Os experimentos foram realizados em forma comparativa empregando-se eletrodos de ouro policristalino e monocristalinos de orientações (111) e (210). Para as superfícies monocristalinas, os resultados de reflectância confirmam o significativo efeito da orientação cristalográfica durante a deposição e redissolução do chumbo sobre as diferentes superfícies de ouro estudadas. O trabalho mostra que a existência de diferentes tipos de estruturas para o chumbo adsorvido depende não só da distribuição atômica do substrato mas acima de tudo do potencial aplicado. Adicionalmente, é feita uma tentativa para explicar o comportamento do ouro policristalino com base nos resultados obtidos para os dois monocristais pesquisados.

The underpotential deposition of lead on gold has been studied by cyclic voltammetry and UV-visible differential reflectance spectroscopy. Comparative experiments were carried out with a polycrystalline gold electrode and two single-crystal gold electrodes with the orientations (111) and (210). For the single crystal surfaces, the reflectance results confirm the large effect of the crystallographic orientation on the deposition and redissolution of lead on gold surfaces. The existence of different types of structures for adsorbed lead, depending not only on the atomic distribution of the substrate but above all on the electrode potential, is demonstrated. An attempt is made to explain the behavior of polycrystalline gold on the basis of the results obtained for the two investigated gold single crystal faces.

Keywords: *underpotential deposition, gold single crystals, spectroelectrochemistry, UV-visible differential reflectance spectroscopy*

Introduction

Electrocatalytic processes are widely studied, firstly to understand better their reaction mechanisms, secondly to improve industrial applications. The reaction mechanisms can be studied by modifying the structure of the electrode surface in order to influence the adsorption of the different species involved in the electrocatalytic processes. One way of modifying a catalytic metallic surface is to deposit a second metal on it by a galvanostatic, potentiostatic or electroless procedure. Bulk metal deposition is preceded by the gradual build-up of a monolayer, or of a submonolayer, at potentials more positive than the reversible Nernst potential of the bulk deposition, in what is called underpotential deposition (upd).

In upd the adsorbate-substrate interactions are stronger than the adsorbate-adsorbate ones. Obviously, foreign atoms influence the catalytic properties of the surface[1]. The thermodynamic, kinetic and structural aspects of the upd of lead on gold surfaces have been the subject of many studies[2-9] which have demonstrated the strong dependence of the adsorption behavior of lead on the crystallographic orientation of the gold substrate[8,9]. Additionally, it was observed that coadsorption phenomena are absent in the underpotential range and that lead upd on single crystal gold surfaces can be well described by the ideal monolayer model[5]. The behavior of lead upd on a polycrystalline gold surface was similar to that on an Au(110) surface, which was explained by a possible predominance of (110) regions. It was confirmed that the deposition of lead on the (111) face and its removal were irreversible processes[8].

The aim of the present work is to investigate the Au/Pb system by using *in situ* UV-visible differential reflectance spectroscopy (UVDRS) in the wavelength range 350 to 750 nm, during a cyclic voltammogram[10-12]. Polycrystalline Au and Au(h,k,l) electrodes in 10 mM $HClO_4$ + 1 mM $Pb(ClO_4)_2$ solutions were studied. The gold single crystal faces chosen were the (111) and (210) planes in order to establish the spectroscopic behavior of two distinct single crystal orientations which exhibit a totally different electrochemical behavior[8] and to compare them with polycrystalline gold.

Experimental

The electrochemical set-up consisted of a Wenking MP81 potentiostat, a X-Y recorder and a three-electrode, one-compartment cell. The polycrystalline gold electrode was prepared by melting a 99.95% gold wire in a graphite crucible with cylindrical internal shape. One of its faces (geometric area 0.166 cm^2) was polished to a mirror finish. For the single crystals, all operations of crystal growth, orientation, cutting of individual faces and surface preparation were carried out at CNRS Meudon[13]. Just before their introduction into the cell, the electrodes were flame treated, cooled in ultra pure water and protected with a drop of water before their transfer to the electrochemical cell. The counter electrode was a gold wire which was also flame treated before immersion into the cell. All potentials were measured with respect to a commercial mercury-mercurous sulfate electrode (MSE) connected to the main compartment of the cell by a glass bridge elongated by a Luggin capillary.

The 10 mM $HClO_4$ + 1 mM $Pb(ClO_4)_2$ solutions were prepared with Suprapur grade acid and p.a. grade salt (both from Merck), and ultrapure water from a Millipore Milli Q system. All experiments were performed at room temperature.

The spectroelectrochemical technique used combines cyclic voltammetry and reflectance measurements, collecting spectra every few milliseconds and then calculating difference spectra between the averaged absorbance curves recorded at two different potentials. This procedure is indicated for systems in which the spectra at different potentials present only small changes. The potential dependence of the absorbance is a very powerful way to observe the formation of layers at electrode surfaces, as already shown for superficial oxides[14]. The optical equipment used consisted of a Harrick RSS-C rapid-scan spectrometer[10]. The light, from a quartz-halogen lamp, falls on a grating mounted on the mobile frame of a small galvanometer shaft and is split into a reference and a sample beam and collected by two identical Hamamatsu R955 photomultipliers. The resulting output signals are processed and averaged, and stored in a Nicolet 370 data acquisition system connected to a personal computer as $\Delta R/R$ (= $(R_2 - R_1)/R_1$ where R_1 is the reference beam signal and R_2 is the reflected sample beam). The data treatment was made with a specific software, as described elsewhere[10], which allows the calculation of the absorbance, A, as -log ($\Delta R/R$ + 1) and the presentation of three-dimensional diagrams (absorbance-wavelength-potential). The electrochemical control of the system was made with the same potentiostat used in the voltammetric experiments and the cell used had a quartz cylindrical compartment with a glassy-carbon counter electrode of *ca.* 2 cm diameter and with a MSE reference electrode. The working electrodes were mounted in a syringe to facilitate their positioning into the cell and they were flame treated, as described above for the electrochemical experiments.

Two kinds of UVDRS experiments were carried out, one by taking spectra at fixed potentials at the values corresponding to the different upd peaks, and the other by taking spectra during a cyclic voltammogram (CV) at 2 mV s^{-1}. The wavelength range was from 350 to 750 nm. Two two-dimensional presentations are possible: the dependence of the absorbance change, ΔA (which is equal to the difference between the absorbance at a given potential and the absorbance at a reference potential) at a fixed wavelength (reflectogram) on the applied potential, and the dependence of A on the wavelength at a fixed potential (spectrum)[10]. In this work the spectra are also displayed in three-dimensional diagrams as (ΔA, λ, E).

Results

Gold (111)

The CV for lead upd on Au(111) shows five pairs of peaks, in agreement with that obtained by Hamelin[8] using $HClO_4$ + PbF_2 (Fig. 1). The cathodic peaks are labeled as follows: A1 = -0.36; A2 = -0.40; A3 = -0.52; A4 = -0.59; A5 = -0.65 V/MSE and the anodic peaks as follows: D1 = -0.205; D2 = -0.29; D3 = -0.36; D4 = -0.58; D5 = -0.62 V/MSE. According to literature[9], peaks A1 and A2 could

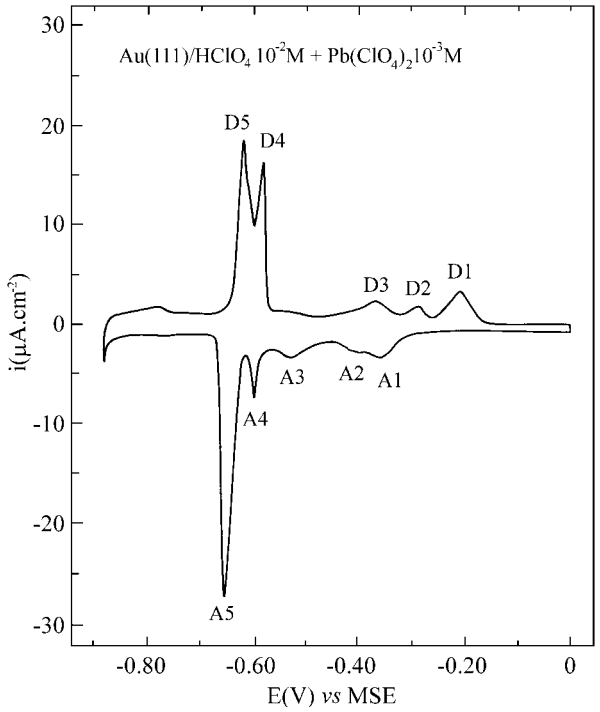

Figure 1. Cyclic voltammogram of Au(111) in 10 mM $HClO_4$ + 1 mM $Pb(ClO_4)_2$ recorded at 10 mV s^{-1} in the potential range from 0 to -0.88 V *vs.* MSE, temperature ≈ 25 °C.

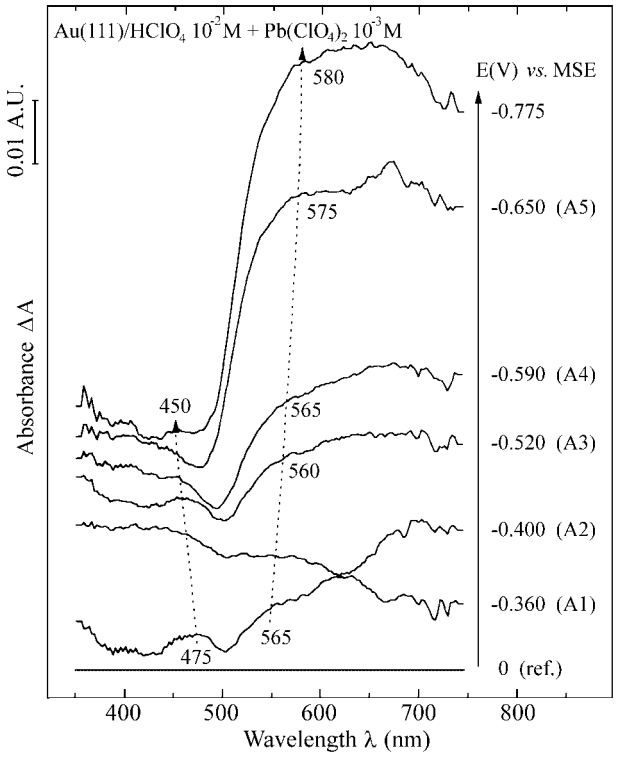

Figure 2. UV-visible differential reflectance spectra of Au(111)/10 mM $HClO_4$ + 1 mM $Pb(ClO_4)_2$ at the fixed potentials shown (reference spectrum taken at 0 V/MSE).

be related either to a substrate modification by lead adsorption or to the adsorption of lead on the substrate surface defects. Peak A3 could be identified as corresponding to the p(1x1) structure, peak A4 as displaying the p($\sqrt{3}$ x $\sqrt{3}$) 30° geometry and peak A5 as corresponding to the p($\sqrt{28}$ x$\sqrt{28}$)18°90' structure. An adsorption isotherm has been used to describe lead upd on Au(111)[5]; at the potential of peak A5 over a range of just about 50 mV, the coverage increased dramatically from θ ≈ 0.4 to θ ≈ 0.9, which was interpreted as a transition between the p($\sqrt{3}$ x $\sqrt{3}$)30° and the p($\sqrt{28}$ x$\sqrt{28}$)18°90' structures of the lead submonolayer[5].

Figure 2 shows UV-vis differential spectra for the Au(111)/Pb interface at fixed potentials corresponding to the cathodic peaks (deposition of lead), with the spectrum at 0 V/MSE as reference. In Fig. 3 the differential spectra, obtained during the negative (Fig. 3a) and positive (Fig. 3b) sweeps of the potential at a rate of 2 mV s^{-1} are shown. Comparing Figs. 2 and 3 one can see that the spectra taken at the fixed potential condition (Fig. 2) present a better definition of the bands than those taken during a potential sweep (Fig. 3). So, while in Fig. 2 there is a noticeable absorbance change at λ > 475 nm already at E = -0.52 V (peak A3), in Fig. 3 a similar change of the absorbance occurs only at E ≤ -0.68 V (peak A5).

Comparing Figs. 3a and 3b, it can be observed that lead upd is fairly reversible. In the positive potential sweep, at λ > 500 nm and E < -0.58 V, the spectra obtained begin to show a better definition of the bands at 575 and 670 nm. After plotting the spectra of Fig. 3 at different potentials, and rotating the xy plane by π/2, we obtain the 3D spectra of Au(111)/Pb displayed in Fig. 4. In the wavelength region between 350 and 525 nm, the absorbance decreases during the deposition and increases during the dissolution of lead. On the contrary, above 525 nm the absorbance increases during the deposition and decreases during the dissolution of lead. It can be seen that after a potential cycle the spectra has changed slightly, since the final spectrum is not a horizontal line of zero absorbance.

At this point, it can be concluded that the UV-vis differential spectra suggest a strong change in the electrode coverage at E < -0.58 V and, due to the difference between the adsorption/deposition and dissolution/desorption kinetics, the bands at 575 and 670 nm are more defined during the positive potential sweep.

Gold (210)

Lead upd on Au(210) presents three pairs of peaks (Fig. 5) in agreement with Ref. 8, but the reversibility is slightly different. Peaks are labeled as follows : A1 and D1 = -0.38; A2 and D2 = -0.645 and A3 and D3 = -0.795 V/MSE. The middle peaks A2 and D2 are smaller than the other two peaks. As pointed out by Hamelin and Lipkowski[9], the

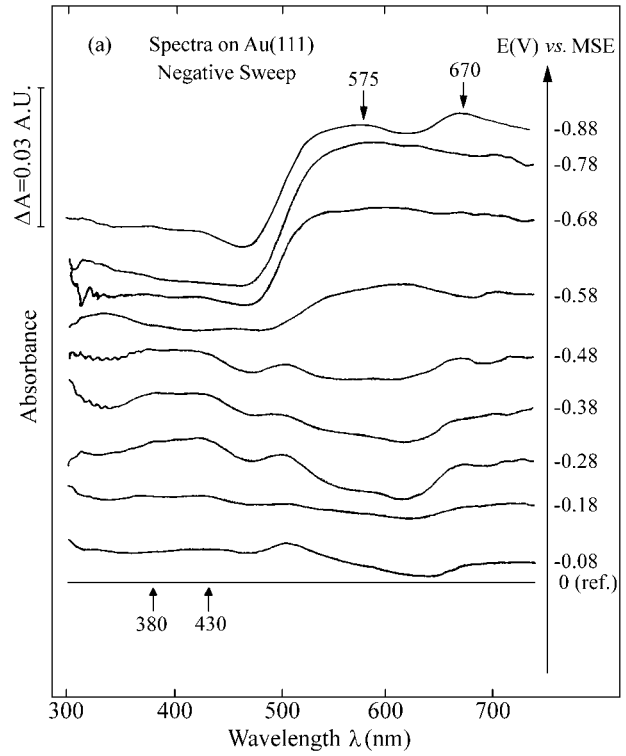

Figure 3a. Two-dimensional UV-visible differential reflectance spectra corresponding to the deposition of lead on Au(111) in 10 mM $HClO_4$ + 1 mM $Pb(ClO_4)_2$ solution during a negative potential sweep from 0 to -0.88 V/MSE, at 2 mV s^{-1}, temperature ≈ 25 °C (reference spectrum taken at 0 V/MSE).

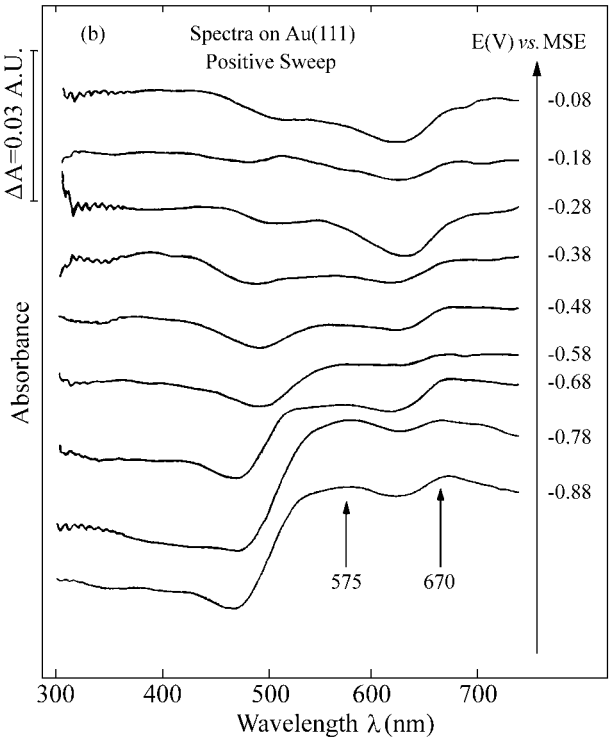

Figure 3b. Two-dimensional UV-visible differential reflectance spectra corresponding to the dissolution of lead on Au(111) in 10 mM $HClO_4$ + 1 mM $Pb(ClO_4)_2$ solution during a positive potential sweep from -0.88 to 0 V/MSE, at 2 mV s^{-1}, temperature ≈ 25 °C (reference spectrum taken at 0 V/MSE).

number, the amplitude, and the width of the peaks in the cyclic voltammograms are related to the atomic arrangement of the crystallographic face of the metal substrate. Additionally, it was shown in LEED experiments[9] that the different intensities of the peaks are associated with discrete changes in the structure of the lead deposit. In the specific case of the face (210), which is a turning point of the (110)-(100) zone, the changes of the structure related to the current peaks in the CV seem to be closer to those corresponding to the (110) face[9].

Figure 6 shows UV-vis differential spectra for the Au(210)/Pb system at the potentials of the deposition peaks. It is possible to distinguish three types of spectra corresponding to the three pairs of peaks (A1/D1, A2/D2, and A3/D3). For peaks A1/D1, at -0.38 V/MSE, the spectrum presents two main bands at 575 and 660 nm. These two bands shift to 520 and 605 nm for peaks A2/D2, at -0.645 V/MSE. Then, the width and the amplitude of the absorption bands increase considerably for the peaks A3/D3, as for the Au(111)/Pb system. Such an increase in the amplitude of the bands can be interpreted in the same way as for the previous system.

The spectra in Figs. 7a and 7b were obtained during a CV at 2 mV s^{-1} for the deposition and dissolution of lead,

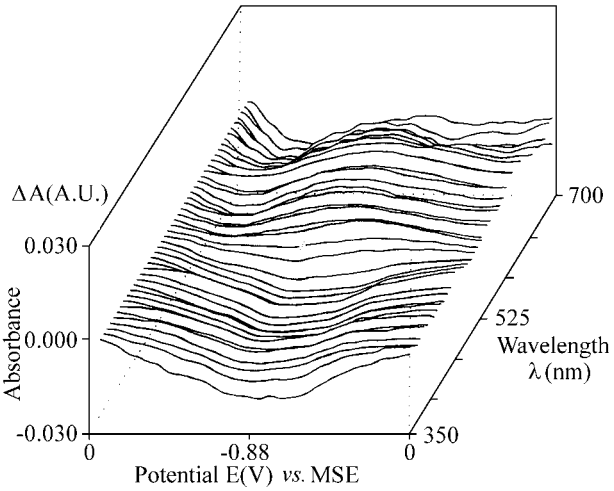

Figure 4. Three-dimensional diagrams obtained from Figs. 3a and 3b during the upd of lead on Au(111) in 10 mM $HClO_4$ + 1 mM $Pb(ClO_4)_2$ solution in the potential range from -0.88 to 0 V/MSE, temperature ≈ 25 °C (reference spectrum taken at 0 V/MSE).

respectively. The bands appearing at $\lambda > 475$ nm for the Au(210)/Pb system are somewhat narrower than those for the Au(111)/Pb system shown in Figs. 3a and 3b. As observed before for Au(111), the spectra in Fig. 7b, corre-

sponding to the positive potential sweep, present a better definition of the bands at 520 and 600 nm between -0.88 and -0.38 V than in the negative potential sweep (Fig. 7a). This observation confirms that there are differences be-

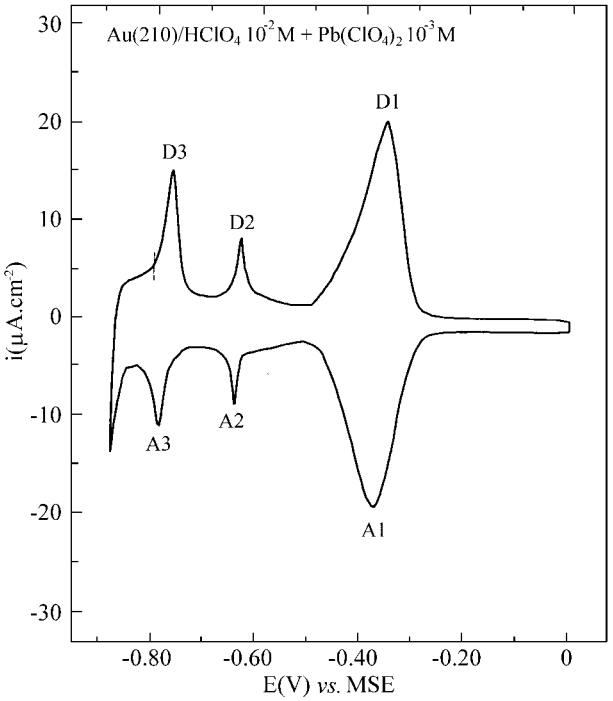

Figure 5. Cyclic voltammogram of Au(210) in 10 mM $HClO_4$ + 1 mM $Pb(ClO_4)_2$ at 10 mV s^{-1} in the potential range from 0 to -0.88 V *vs.* MSE, temperature ≈ 25 °C.

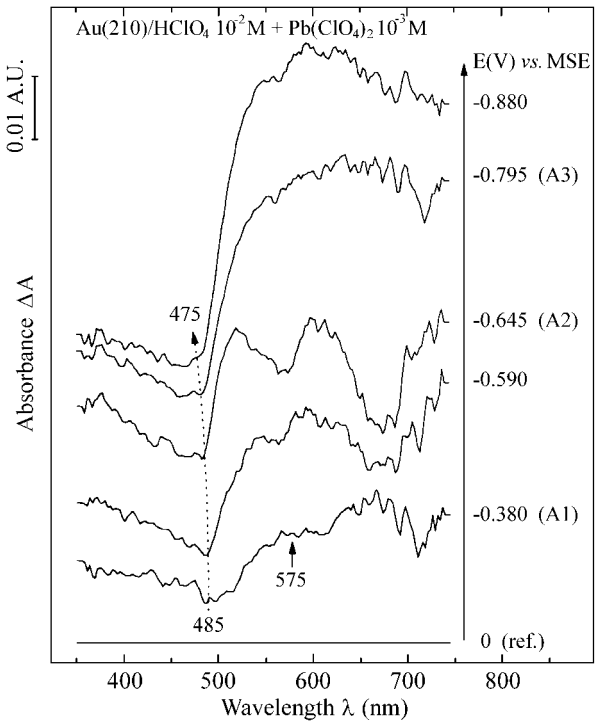

Figure 6. UV-visible differential reflectance spectra of Au(210)/10 mM $HClO_4$ + 1 mM $Pb(ClO_4)_2$ at the fixed potentials shown (reference spectrum taken at 0 V/MSE).

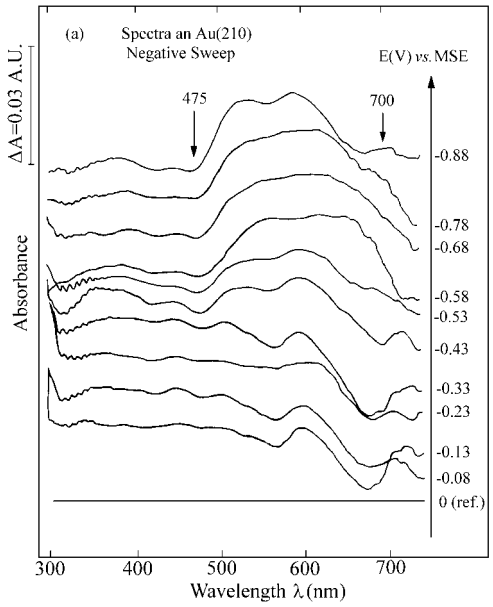

Figure 7a. Two-dimensional UV-visible differential reflectance spectra corresponding to the deposition of lead on Au(210) in 10 mM $HClO_4$ + 1 mM $Pb(ClO_4)_2$ solution during the negative potential scan between 0 and -0.88 V/MSE, at 2 mV s^{-1}, temperature ≈ 25 °C (reference spectrum taken at 0 V/MSE).

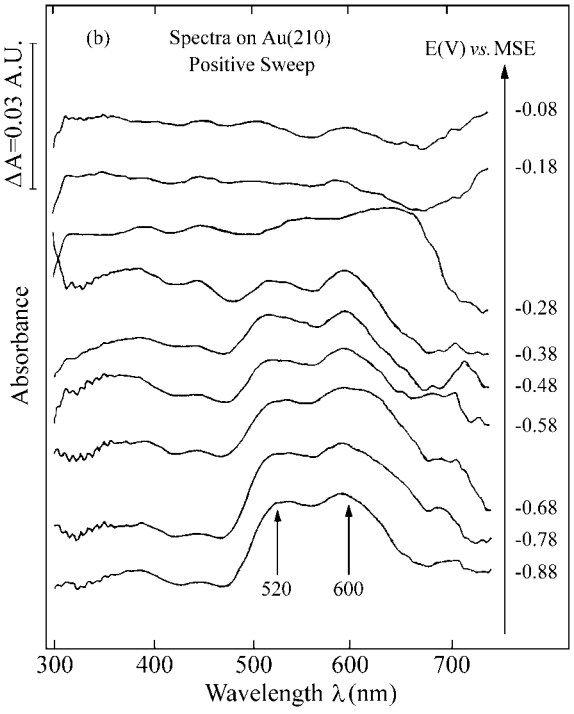

Figure 7b. Two-dimensional UV-visible differential reflectance spectra corresponding to the dissolution of lead on Au(210) in 10 mM $HClO_4$ + 1 mM $Pb(ClO_4)_2$ solution during the positive potential scan between -0.88 and 0 V/MSE, at 2 mV s^{-1}, temperature ≈ 25 °C (reference spectrum taken at 0 V/MSE).

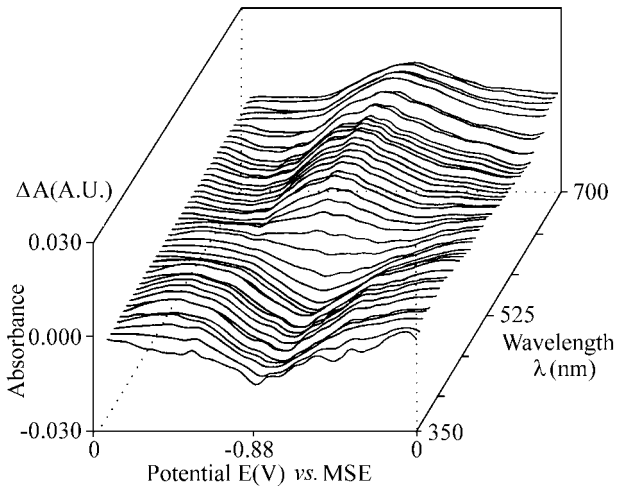

Figure 8. Three-dimensional diagrams obtained from Figs. 7a and 7b during the upd of lead on Au(210) in 10 mM $HClO_4$ + 1 mM $Pb(ClO_4)_2$ solution in the potential range from -0.88 to 0 V/MSE, 25 °C (reference spectrum taken at 0 V/MSE).

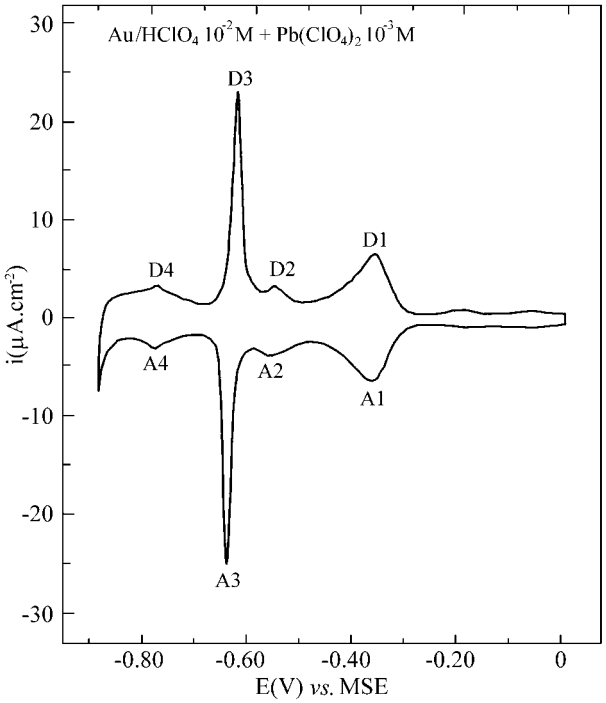

Figure 9. Cyclic voltammogram of a polycrystalline gold electrode in 10 mM $HClO_4$ + 1 mM $Pb(ClO_4)_2$ recorded at 10 mV s^{-1} in the potential range from 0 to -0.88 V vs. MSE, temperature ≈ 25 °C.

tween the processes of deposition and dissolution of lead which can be related to intrinsic changes of the structure of the deposit and/or changes in the kinetic parameters. As it can be seen in the 3D spectra presented in Fig. 8, for the (210) face the spectra have the same general features of the (111) face. However, the relative changes in absorbance with potential are more pronounced for the (210) face, as can be observed from a comparison of Figs. 8 and 4. The

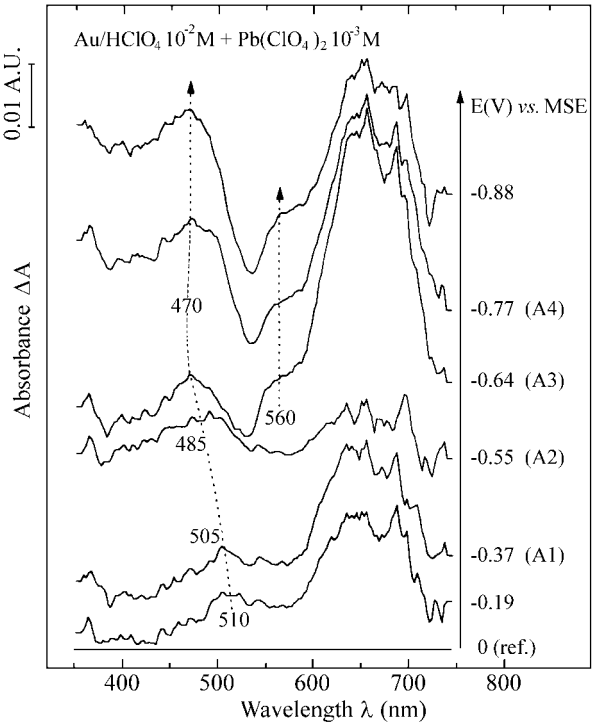

Figure 10. UV-visible differential reflectance spectra of polycrystalline Au / 10 mM $HClO_4$ + 1 mM $Pb(ClO_4)_2$ at the fixed potentials shown (reference spectrum taken at 0 V/MSE).

deposition-dissolution process is not wholly reversible as far as the spectra are concerned, since, as mentioned for Au(111), the last spectrum in Fig. 8 is not a horizontal line of zero absorbance.

Polycrystalline gold

The cyclic voltammogram at 10 mV s^{-1} for polycrystalline gold in an acidic solution containing lead, in the potential range from 0 to -0.88 V/MSE, shows four pairs of peaks (Fig. 9). All processes are rapid, except that corresponding to the pair of sharp peaks A3 and D3, which has a peak separation of about 20 mV. This behavior is quite similar to that observed before[5], but for a slight difference in the intensity of the peaks, probably due to the difference in solution composition. According to Engelsmann *et al.*[5], the behavior of a polycrystalline gold substrate for lead upd is almost the same as that of Au(110). Then, the present results can be interpreted on the basis of the assumptions made by Hamelin and Lipkowski on cyclic voltammetric results and LEED results[9]. For instance, peak A1 at -0.37 V/MSE was attributed to a p(1x1) structure and peak A4 at -0.77 V/MSE to a p(4x4) structure. Peaks A3 at -0.64 V/MSE and D3 at -0.62 V/MSE were attributed to a transformation of the structure of the lead submonolayer, perhaps due to the presence of (111) facets present in the surface. The intensity and potential of peaks A3-D3 coincide with those of peaks A5 and D5 for Au(111)[5,9] (Fig. 1),

which reinforces the last assumption. Thus, it can be proposed that the structure of lead on the polycrystalline gold surface could present a p($\sqrt{28}$ x $\sqrt{28}$)18°90' geometry, or one very close to it, before it changes to a p(4x4) structure.

Figure 10 shows the UV-vis differential spectra at the potentials of the peaks observed in Fig. 9. The spectrum at 0 V/MSE was also used as reference. A small band shifts from 510 to 470 nm with decreasing potential. For $\lambda > 510$ nm the spectra are basically the same, but for the shoulder at 560 nm at potentials more negative than -0.64 V. Additionally, there is a large increase of absorbance at E = -0.64 V (peak A3).

Discussion

Two points are worth discussing. The first one concerns the interpretation of the behavior of polycrystalline gold in the light of the results obtained with single crystal faces. In other words, the question is whether, optically, the polycrystal behaves as a weighted contribution of elementary crystallites of definite orientation. The second point concerns the adsorption states of the lead adatoms on the gold surface. It is important to understand if the optical response in the UV-visible range provides information on the type of substrate sites which are occupied by Pb adatoms and if there is a structural dependence of the upd process.

Optical behavior of lead adatoms on polycrystalline gold as compared to single crystals

A comparison of the spectra for the deposition of lead on polycrystalline gold (Fig. 10) with those for Au(111) (Fig. 2) and Au(210) (Fig. 6), shows that a lead submonolayer on single crystal faces absorbs over a much wider wavelength range (roughly from 480 to 720 nm) than on the polycrystal electrode (600 to 720 nm). Conversely, the intensity of the bands is about 40% greater on the polycrystal (ΔA_{max} of about 0.047 A.U. at peak A3) than on single crystals, where ΔA_{max} is only 0.033 and 0.030 A.U. on the (111) and (210) planes, at peaks A5 and A3, respectively.

However, looking carefully at Fig. 10 (polycrystal) and Fig. 2 (the (111) plane) it is interesting to note that in the negative potential sweep negative bands, corresponding to an increase of reflectance, are seen at around 530 nm in the former and 510 nm in the latter. No similar bands are seen with Au(210). Interestingly, peak A3 for the polycrystal and peak A5 for Au(111) occur at about the same potential, -0.65 V. As noted above, it is at these peaks that the reconstruction of the lead submonolayer is supposed to occur, leading to a change from a p($\sqrt{3}$ x $\sqrt{3}$)30° to a p($\sqrt{28}$ x $\sqrt{28}$)18°90' pattern[9]. At the same time the surface coverage increases dramatically, so that it becomes clear that the negative peaks of the UVDRS spectra result from a decrease of the number of free gold sites (*i.e.*, not covered by lead) near -0.60 V/MSE and consequently a decrease of the well-known absorption edge at *ca.* 500 nm of metallic gold[1]. As expected, nothing similar is seen with the (210) face.

The adsorption states of Pb adatoms on Au

The spectrum chosen as reference corresponds to a well defined electrochemical state of the interface with no upd lead adatoms, which allows us to determine the formation or the disappearance of structures at the electrochemical interface.

The shapes of the UV-vis differential spectra during the upd of Pb on Au are similar and prove clearly the existence of at least two states of Pb on the substrate (Figs. 2, 6 and 10), namely, the submonolayer of Au-Pb_{ads} and the complete layer of Pb_{ads} which corresponds to the final structure -Pb_{ads}-Pb_{ads}-.

At potentials higher than -0.35 V/MSE the differential spectra practically show no bands. Submonolayers of Pb_{ads} species predominate for polycrystalline gold between -0.19 and -0.55 V/MSE, for Au(111) between -0.36 and -0.59 V/MSE and for Au(210) between -0.38 and -0.64 V/MSE. The spectra of Au(111) and Au(210) (Figs. 2 and 6) show little absorption below 470 nm and a progressive increase of absorbance at wavelengths above 500 nm. An increase of the absorbance at lower potentials is likely to correspond to a restructuring and a redistribution of the Pb_{ads} atoms on the gold surface, forming multiple bonds between the Pb_{ads} species like on a metallic surface. This adsorbed state is more defined for single crystals like Au(111) and Au(210). The very sharp (i-E) peaks, according to the Frumkin isotherm model, denote strong lateral interactions between adsorbates, *i.e.*, of -(Pb_{ads}- Pb_{ads})- type.

Finally, the UV-vis spectra (Figs. 3 and 7) show a fair reversibility of the reconstruction process of the lead layer on gold between -0.88 and -0.58 V/MSE.

Conclusions

This UVDRS study of the Au/Pb interface completes and confirms some assumptions obtained from CVs about the occurrence of different adsorption states of lead on a gold surface and the dependence of the surface coverage on the electrode potential. In particular, it can be deduced from the UV-vis spectra that the changes of surface coverage by an adsorbed species lead to large changes of the amplitude of absorption bands.

By comparing the spectra obtained with the two Au single crystal faces studied here with those of the gold polycrystal, it becomes clear that the reconstruction processes affecting the lead submonolayer are very similar for the polycrystal and for the (111) face.

All the results obtained here demonstrate the high sensitivity of the UVDRS technique for detecting small changes of reflectivity due to the presence of an adsorbed layer, even at low coverage.

Acknowledgments

The authors thank Dr. A. Hamelin from LEI / CNRS for preparing the gold single crystals. This work was supported by a bilateral exchange program between CNPq (Brazil) and CNRS (France).

References

1. Kolb, D.M. In Advances in Electrochemistry and Electrochemical Engineering, vol. 11, Gerischer, H.; Tobias, C.W., eds.; Wiley, New York, 1978.
2. Adzic, R.R.; Yeager, E.; Cahan, B.D. *J. Electrochem. Soc.* **1974**, *21*, 474.
3. Schultze, J.W.; Dickertmann, D. *Surf. Sci.* **1976**, *54*, 489.
4. Hamelin, A. *J. Electroanal. Chem.* **1979**, *101*, 285.
5. Engelsmann, K.; Lorenz, W.J.; Schmidt, E. *J. Electroanal. Chem.* **1980**, *114*, 1.
6. Engelsmann, K.; Lorenz, W.J.; Schmidt, E. *J. Electroanal. Chem.* **1980**, *114*, 11.
7. Hamelin, A.; Katayama, A. *J. Electroanal. Chem.* **1981**, *117*, 221.
8. Hamelin, A. J. Electroanal. Chem., **1984,** 165, 167.
9. Hamelin, A.; Lipkowski, J. *J. Electroanal. Chem.* **1984**, *171*, 317.
10. Rakotondrainibe, A.; Spinelli, A.; Lamy, C.; Beden, B. *Spectroscopy Europe* **1993**, *5*, 20.
11. Collas, N.; Beden, B.; Léger, J-M.; Lamy, C. *J. Electroanal. Chem.* **1985**, *186*, 287.
12. Kolb, D.M. In Spectroelectrochemistry, Theory and Practice, Gale, R.J., ed.; Plenum Press, New York, 1988.
13. Hamelin, A. In Modern Aspects of Electrochemistry, Vol. 16, Conway, B.E.; Bockris, J.O'M.; White, R., eds.; chapter 1, p. 1, Plenum Press, New York, 1985.
14. Hahn, F.; Beden, B.; Croissant, M.J.; Lamy, C. *Electrochim. Acta* **1986**, *31*, 335.

FAPESP helped in meeting the publication costs of this article